Journal of Solid Mechanics Vol. 8, No. 1 (2016) pp. 130-151

Dynamic Analysis of Offshore Wind Turbine Towers with Fixed Monopile Platform Using the Transfer Matrix Method

M. Feyzollahzadeh , M.J. Mahmoodi *

Faculty of Mechanical and Energy Engineering, Shahid Beheshti University, Tehran, Iran

Received 15 November 2015; accepted 13 January 2016

ABSTRACT

In this paper, an analytical method for vibrations analysis of offshore wind turbine towers with fixed monopile platform is presented. For this purpose, various and the most general models including CS, DS and AF models are used for modeling of wind turbine foundation and axial force is modeled as a variable force as well. The required equations for determination of wind turbine tower response excited by the Morrison force are derived based on Airy wave theory. The transfer matrix is derived for each element of the tower using Euler-Bernoulli's beam differential equation and the global transfer matrix is obtained considering boundary conditions of the tower and constructing the point matrix. The effective wave force is intended in several case studies and Persian Gulf Environmental conditions are examined for the installation of wind farms. Finally, the obtained results by the transfer matrix method are compared with the results of the finite elements method and experimental data which show good agreement in spite of low computational cost.

Keywords : Offshore wind turbine tower; Transfer matrix method; Natural frequencies; Foundation models; Morrison wave force.

1 INTRODUCTION

THE offshore wind turbine technology have advanced in recent years [1,2] and some of countries such as Netherlands, Denmark and Sweden have long-term programs to installation of wind farm [3]. Some researchers have been also done about the feasibility study of utilizing offshore wind turbine in Iran and the studies are suggestive of Iran shores especially Persian Gulf have potential of installation offshore wind turbine with fixed monopile platform [4-7].

Determination of the dynamic response of a wind turbine tower under external forces is an important step in stress and fatigue analysis of the wind turbine structural design that should be quite accurate [8]. Low-accurate modeling of the tower leads to predict incorrect response of the tower and improper estimation of stress [9]. On the other hand, increasing wind velocity, waves induced forces, water stream force etc. give rise to offshore turbine towers are exposed to more difficult conditions than offshore turbines [10,11]. So far, many researches have been done in these fields which usually have used the finite element method (FEM). The FEM has traditionally been used in the development of wind turbine structures mainly to investigate the global behaviors in terms of frequencies, mode shapes, top deflection, and global stress/strain levels [11,12].

Bazeos et al. used the FEM to static and stability analysis of the wind turbine tower [13]. Salehi and his co-workers used the FE based Ansys software to static analysis of offshore wind turbine tower under the thrust force

*Corresponding author. Tel.: +98 21 73932667.
E-mail address: mj_mahmoudi@sbu.ac.ir (M.J.Mahmoodi).

[14]. In [15] another study was conducted under Lavassas's supervision in which researchers obtained the dynamic response of the tower subjected to wind force. Later, Jianyuan et al. analyzed the dynamic response of the tower induced by turbulence wind force in the Ansys software [16]. Bush and Manuel studied the effects of three foundation models in the Fast software and showed that distributed springs foundation model is higher accuracy than other of foundation models [17]. In [18], the authors by using the Morison equation and the Airy wave theory obtained the response of the offshore wind turbine tower to the wave force in the Fast software. The results of these papers indicated that the FEM usually predicts response of the offshore wind turbine tower and related stresses with a good accuracy nevertheless the method is a time consuming process and this issue is clearly visible in the detailed analysis [19].

On the other hand, analytical method used for calculating natural frequencies and response of wind turbine towers have been previously presented. In [20] Murtagh and his co-workers provided simple analytical method to determine natural frequencies and mode shapes by using a constant cross-sectional area. Maalawi proposed some explicit functions for cross-section and moment of inertia of the wind turbine tower and solved the differential equation of motion in the tower torsional vibrations [21]. Wang et al. used the theory of thin-walled beams and studied the free vibration of wind turbines towers [22]. However, studies in this area have been used for specific models, the results indicate that the differential equation of the offshore wind turbine tower does not possess analytical solution in general and numerical methods would be employed to solve.

Among the analytical procedures transfer matrix method (TMM) is simple and accurate method that used to analyze the vibration of beams and other structures [23-25]. In fact, the TMM is a form completed of Hoelzer's procedure which was presented to study torsional vibrations of shafts in 1921 [26]. Later, Myklestad applied the Hoelzer method with a little change for transverse vibrations of beams [28]. Pestel et al. focused their research on the review and expansion of the TMM and the results of research finally published in [28]. Dai and colleagues used this method to study the three-dimensional vibrations of the pipes [29]. Orasanu and Craifaleanu obtained natural frequencies of a beam with a constant cross section and a central point mass and results from the TMM compared with FEM and experimental data. Orasanu and Craifaleanu showed that in vibration analysis of a beam with a concentrated mass, the TMM has higher accuracy with respect to the FEM [30].

The transfer matrix method has some advantages in computer implementation [31-33] including ease of software design, small memory supplies and obtainability of ready-made transfer matrix catalogues for different elements. On the other hand, in TMM, accuracy of results raised by increasing the number of elements and also, the determinant of the characteristic equation does not depend on the number of elements unlike the FEM [34, 35]. In addition, the TMM can be used as an analytical method; therefore, this method contains merely sources of discretization errors [36]. It should be noted that the TMM includes some limitations which have prevented extension of TMM unlike the FEM. In the high modes, transfer matrix method contains numerical difficulties which lead to inaccurate determination of the natural frequencies [33].Therefore transfer matrix method is suitable for systems in which low vibration modes are dominant in the design. Also, in many cases when a very stiff spring exists between two elements or in the presence of joint with high flexibility, natural frequencies determination using the transfer matrix method would be difficult [28].

In wind turbine tower design, the natural frequencies of the first and second vibration modes are often required and the third frequency is rarely used [2]. On the other hand, equivalent foundation springs with high stiffness exist in wind turbine towers modeling. Nevertheless, the springs are taken into account at the base of the tower, thus the analysis excludes difficulty in applying the transfer matrix method despite possessing springs at the tower base. These items direct some researchers use the TMM in static and dynamic analysis of wind turbine towers in the recent years. Meng et al. studied the buckling of the wind turbine tower by using the TMM [37]. They wrote another paper and applied the TMM to calculate natural frequency of wind turbine towers with a fixed fulcrum regardless of the axial force [38]. Support of wind turbine towers in reality has a finite stiffness. Therefore, considering the fully clamped model for wind turbine tower foundation is not suitable [39]. On the other hand, offshore turbines are installed in more soft ground; hence, modeling of offshore turbines support is very significant. Furthermore, sometimes, the weight of offshore towers is more than the weight of the Nacelle weight [17]. Thus, neglecting of the axial force variations leads to erroneous results. Consequently, results of the modeling would be close to the actual value when axial force is modeled as a variable force and support of the tower is speculated as an elastic fulcrum.

All of the researches that have been carried out so far can be divided into two broad categories: The first category includes articles that presented an analytical method for the vibrations of wind turbine towers however, they were associated with simplifications and regardless of the axial force variations and modeling foundation [20, 37, 38] or presented for specific models [20-22]. The second category contains papers in which accurate modeling of wind turbine towers have been discussed and numerical methods especially the finite element method has been used [11-18]. In this paper, by using the TMM, the analytical solutions for forced vibration of offshore wind turbine

tower with variably distributed axial loads and elastic foundation are found. For this purpose, the wind turbine tower foundation is modeled using the DS, AF and CS standard models. The wind turbine tower is discretized through applying the TMM and by expending the Euler - Bernoulli equation. Transfer matrix is derived for each of the tower elements. Finally, the effective wave force is envisioned in several cases study and the obtained results by the transfer matrix method are validated with the results of the finite elements method.

2 WIND TURBINE DESIGN METHODS

Although wind turbine blades are made with high accuracy but there are always imbalances between the wind turbine blades [11] which leads to excitation load on the wind turbine tower by rotor frequency (1P). Furthermore, each time a blade passes the tower, the shadowing effect raised by wind causes a harmonic load on the structure [12]. For a three-bladed wind turbine, the effect result an excitation on the blade passing frequency 3P as well as multiples thereof for example 3P, 6P, 9P and so on. Another external applied load on the tower is wave load originates from sea states whose frequency is normally about 0.20 to 0.30 Hz [40]. So, the tower frequency must not coincide with the excitation frequencies of the imbalances load, i.e. shadow load and wave load. Hence, three classical design approaches have been defined in the categories of wind turbine design methods as follow [40]:

1. Soft–soft design: the tower frequency is less than 1P.
2. Soft–stiff design: the tower frequency is between the frequencies 1P and 3P.
3. Stiff–stiff design: the tower frequency is higher than the blade passing frequency 3P.

Fig. 1 shows the frequency ranges corresponding to each of the design approaches, schematically. Designing the wind turbine in stiff– stiff approach requires a very stiff foundation leading to an expensive design. Also designing in the soft–soft through high wave loading, might be critical. Designing in the soft– stiff approach is suitable and economic [40]. Hence, most wind turbines towers are designed within the soft– stiff [41] and so in this paper, Soft–stiff design method is examined to study in order to set up a wind farm in the Persian Gulf.

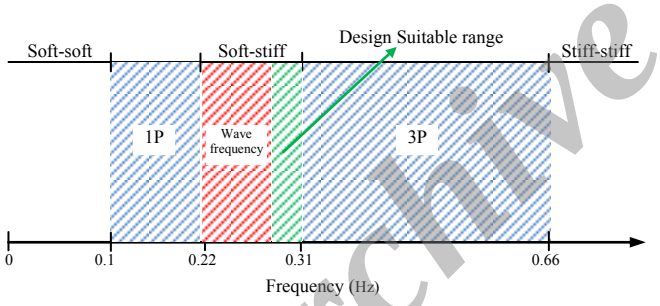

Fig.1
Design frequency range of the offshore wind turbine towers [40].

3 WAVE FORCE

Wave load is one of the main forces on offshore wind turbine structures. This load results from the water flow around the support structure of the wind turbine. Many theories for calculating wave loads are presented according to sea conditions and structural dimensions [42]. Wave loads of slender structures can be described by the Morison's equation. Slender structure can be defined as structure with a small ratio between diameter and wavelength [42]. Consequently, Morison's equation can be used with reasonable accuracy when the dimension of the structure, D is small enough relative to the wavelength, λ namely when the ratio $D/\lambda < 0.2$ [39, 42]. For non-slender structures the diffraction theory must be used for the calculation of wave loads [42]. Commonly, diameter of the monopile in offshore wind turbines is between 3.5 to 6 meters [42, 39]. The wavelength adopts different values proportional to the weather. Although, the mean value of wavelength is about 40 to 80 meters [39]. For example, Table 1. shows the mean wavelength for the two sites Middelgrunden and Rodsand in different situations. If the wavelength is assumed to be 40 m and pile diameter is assumed to be 6 m by dividing greatest value to the least value, the ratio of D/λ is obtained 0.15 that it shows Morison's equation can be used to determine the wind turbine wave load in the public case.

Table 1
The mean wavelength for the two sites Middelgrunden and Rodsand. [39]

Site	Wavelength (*m*)	Wave height (*m*)	Depth (*m*)
Middelgrunden	40	3.8	5.5
	45	3.5	8
	47	3.5	9.5
Rodsand	50	3.5	11
	64	6.2	8
	76	6.7	9.5
	88	6.7	11

By Morison's equation, the horizontal force on the monopile is expressed as [42]

$$Q(\zeta,t) = F_I + F_D \tag{1}$$

where $Q(\zeta,t)$ is the wave force per unit length, ζ is a coordinate along the pile length whose datum is located on the water surface as shown in Fig. 2, F_I is the inertia term of the wave force, F_D is the drag term of the wave force which can be expressed as [42]

$$\begin{cases} F_I = C_M \rho_w \dfrac{\pi D^2}{4} \dfrac{dU}{dt} \\ F_D = \dfrac{1}{2} C_D \rho_w D U \left|U\right| \end{cases} \tag{2}$$

Called the mass coefficient C_M, the water density ρ_w, outer diameter of the pile D, velocity of the water flow U and drag coefficient C_D. In the general case, C_M and C_D depend on the smoothly and roughly of the pile which increased by increasing surface roughness [43]. Several methods to calculate these coefficients are presented in [43-45].

To determine the drag and inertia force, the water flow velocity profile must be specified. For this purpose Airy's wave theory is employed in this paper. Fig. 2 shows characteristics of the Airy's wave. According to Airy's wave theory, the horizontal wave velocity is as follows [42]

$$U = \frac{H}{2} \frac{gT}{\lambda} \frac{\cosh\left[2\pi(\zeta + d_w)/\lambda\right]}{\cosh\left[2\pi d_w/\lambda\right]} \cos\left(\frac{2\pi t}{T}\right), \quad -d_w \le \zeta \le 0 \tag{3}$$

where T stands for the wave period, t is the time, d_w is water depth, H is wave height and λ is wavelength. Substituting Eq. (3) into Eq. (2), the wave force can be expressed as:

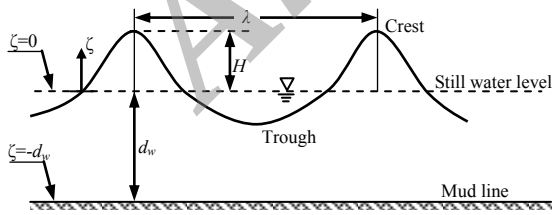

Fig.2
Characteristics of the Airy's wave theory. [42]

$$\begin{cases} F_I = \mathrm{F_I}(\zeta) \sin\left(-\dfrac{2\pi t}{T}\right), \quad -d_w \le \zeta \le 0 \\ F_D = \mathrm{F_D}(\zeta) \left|\cos\left(\dfrac{2\pi t}{T}\right)\right| \cos\left(\dfrac{2\pi t}{T}\right), \quad -d_w \le \zeta \le 0 \end{cases} \tag{4}$$

and $\mathrm{F_I}(\zeta)$ and $\mathrm{F_D}(\zeta)$ are defined as:

$$\begin{cases} \mathrm{F_I}(\zeta)=\left[\dfrac{\pi}{\lambda}\dfrac{\cosh\left[2\pi(\zeta+d_w)/\lambda\right]}{\cosh\left[2\pi d/\lambda\right]}\right], \ -d_w \le \zeta \le 0 \\ \mathrm{F_D}(\zeta)=\dfrac{gT^2}{4\lambda^2}\left(\dfrac{\cosh\left[2\pi(\zeta+d_w)/\lambda\right]}{\cosh\left[2\pi d_w/\lambda\right]}\right)^2, \ -d_w \le \zeta \le 0 \end{cases} \quad (5)$$

4 MODELING OF WINDTURBINE TOWER

4.1 Foundation modeling

To determine the equivalent model for the foundation, structure response to excitation force should be examined then the foundation model is selected based on it. Foundation resists against the pile motion raised by external forces such as wind or wave force. However the foundation does not move or its movement is very little [13]. In this case, the wind turbine tower foundation can be modeled by a series of springs that springs stiffness coefficient is not constant in general and is determined as proportional to the amplitude of the external loads [46]. The accuracy of equivalent spring usage is not suitable in which the ground shake like an earthquake is dominant. In this case, the seismic added mass should be considered together with equivalent springs [13]. Regarding this concern, response of the wind turbine tower is considered merely under the wave load in the present paper. So the equivalent spring is employed for foundation modeling.

Stuttgart institute of wind Energy (SWE) derived three models to signify the monopile foundation as described in Fig. 3, schematically. The figure includes the distributed springs (DS) model, the apparent fixity length (AF) model and the coupled springs (CS) model. The DS model idealizes the monopile with elastic foundation as a free-free beam with horizontal springs distributed along the subsoil share of the monopile. The beam uses the actual properties of the monopile both top and bottom of the mudline including the real diffusion depth. The subsoil spring stiffness constants are depth-dependent and can be extracted using of the horizontal soil resistance versus horizontal monopile displacement (*P*-*y*) data. For this purpose, soil ultimate resistance (P_u) must be determined and employed in the analysis. In general, ultimate resistance is depending on the depth of the foundation, pile diameter and physical conditions of soil. In this paper, wind turbine tower case study is placed on the sand bed and therefore, expressions of the relationships are only required for sand. Soil ultimate resistance for sand is expressed as [47]

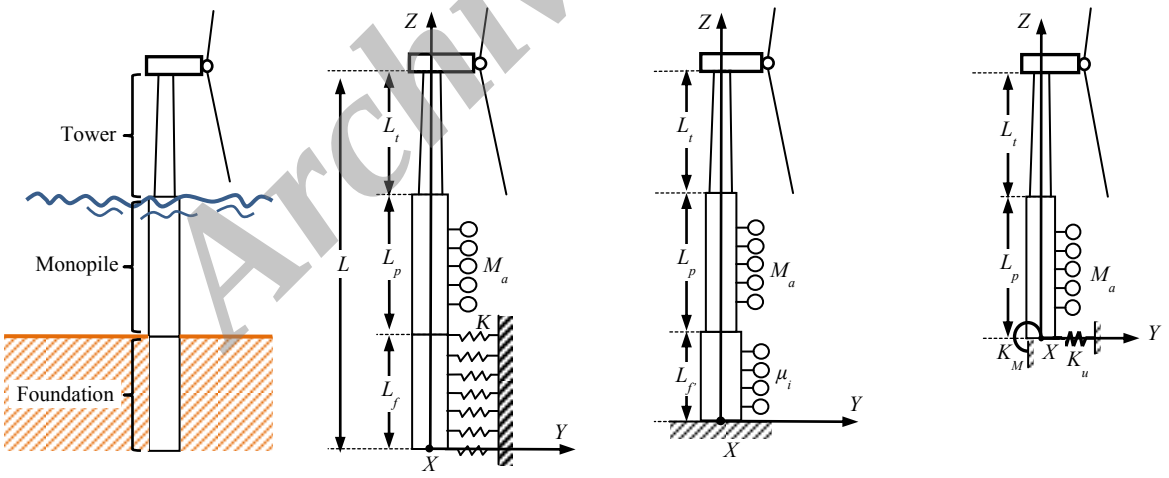

(a) (b) (c) (d)

Fig. 3
Modeli*n*g of offshore wind turbine tower, a) Offshore wind turbine tower, b) DS foundation model, c) AF foundation model, d) CS foundation model.

$$P_u=\min\left\{\left[\left(C_1\times h+C_2\times D\right)\times\gamma\times h\right],\left[C_3\times D\times\gamma\times h\right]\right\} \quad (6)$$

where γ is effective soil weight, h is foundation depth, D is pile diameter and the coefficients C_1, C_2 and C_3 dependent on the angle of internal friction of sand (φ) and can be determined from Figs. 4(a) and 4(b). Soil resistance can be obtained using Eq. (6), as follows [47]

$$\underline{P}(Z) = f \times P_u \times \tanh\left(\frac{k \times h}{A \times p_u} \times v(Z)\right),\ 0 \le Z \le L_f \tag{7}$$

where Z is coordinate axis along the length of tower that measured from the beginning of the foundation and L_f is length of the monopile which is embedded inside the seabed as shown in Fig. 3. Also k is bulk modulus of subgrade reaction and it is dependent on the angle of internal friction of sand and can be determined from the Fig. 4 (c), $\underline{P}(Z)$ stands for the soil resistance; $v(Z)$ is lateral displacement of foundation and f is load factor for cyclic or static condition which is obtained as follows [47]

$$\begin{aligned} f &= 0.9 \quad \text{for cyclic loading} \\ f &= \left(3.0 - 0.8\frac{h}{D}\right) \text{ for static loading} \end{aligned} \tag{8}$$

Finally, the stiffness of the DS foundation model is calculated using the following equation [40]

$$K(Z) = \frac{\underline{P}(Z)}{v(Z)},\ 0 \le Z \le L_f \tag{9}$$

$\underline{P}(Z)$ depends on the external load. So, the stiffness is also dependent on external load and must be determined in accordance with external excitation. For this purpose, shear force and bending moment due to external load must be transmitted to the mudline by determining $P(Z)$, the equivalent stiffness can be calculated.

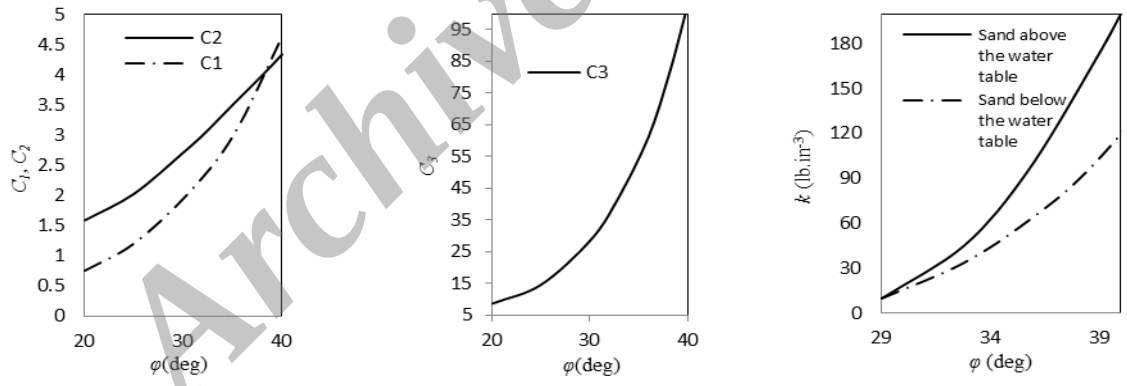

Fig. 4
Determination of the constant coefficients in the DS model, a) coefficients C_1 and C_2, b) coefficient C_3, c) modulus of subgrade reaction. [47]

The AF model idealizes the monopile with elastic foundation as a cantilever beam whose properties vary from top to bottom of the mudline. The beam above the mud line has the actual properties of the monopile and the beam below the mud line has operative properties and a fictive length. To determine the equivalent diameter and equivalent length L_f, results of the $\underline{P}$-y analysis are used and an equivalent beam model of DS model is obtained. For this purpose, analysis program such as LPILE [17] can be used. In according with this program, equivalent diameter and fictive length can be obtained by introducing the soil resistance and the dimensions of the pile. In [48] AF model algorithm specifications have been presented.

The CS model idealizes the foundation compliance as a set of translational and rotational by coupled springs located at the mud line. Above the mud line, the monopile is modeled as a beam with the real properties of the monopile. In this case, the foundation stiffness matrix is calculated using the following equation [48]

$$K = \begin{bmatrix} \frac{12EI_f}{{L_f}^3} & -\frac{6EI_f}{{L_f}^2} \\ -\frac{6EI_f}{{L_f}^2} & \frac{4EI_f}{L_f} \end{bmatrix} = \begin{bmatrix} k_{u,F} & k_{u,M} \\ k_{\theta,F} & k_{\theta,M} \end{bmatrix} \tag{10}$$

where EI_f is foundation bending stiffness.

Among the three presented models, the DS model is more accurate than the other models and if complete information about soil conditions is available, the DS model can be used with high accuracy [46]. AF model is less accurate than the DS model however the computational capacity of the AF model is less than the DS model. It is clear from Eq. (10) that CS model stiffness is independent from the location of installed platform and solely depends on the size of monopile. Therefore, CS model is less accurate than the DS and AF models. CS model can be applied when detailed information is not available for soil installation. In this case, foundation model can be achieved via only the dimensions of the pile. In the following, the equations for each of the three models are discussed.

4.2 Equations of motion

Rotation coefficient (δ) is a measure which indicates the significance of shear deformation on transverse vibration. If the δ value is less than 0.25, both of the Euler-Bernoulli theory and Timoshenko beam theory give the identical results [49]. In offshore wind turbine with monopile platform, this index is calculated as follows [45]

$$\delta = \frac{r}{\sqrt{2}L} \tag{11}$$

where, r is tower radius and L is total length of tower, monopile and foundation. Tower diameter is usually in the range of 3.5 to 6 meters and total length of tower and monopile takes between 120 to 200 meters as well. So, considering the largest numerical value for r taking 3 m and the smallest value for L which is 120 m [42], the rotation rate would be equal to 0.017. Thus, both the beam theories of Euler-Bernoulli and Timoshenko provide the similar results and therefore, in this paper, Euler-Bernoulli beam theory is used for vibration analysis of the tower.

Differential equations of motion of the tower and the monopile, can be obtained as follows [46, 50]

$$\begin{cases} \frac{\partial^2}{\partial Z^2}\left(EI_t(Z)\frac{\partial^2 v}{\partial Z^2}\right)+\frac{\partial}{\partial Z}\left(P(Z)\frac{\partial v}{\partial Z}\right)+\rho_t A_t(Z)\frac{\partial^2 v}{\partial t^2}=0,\ L_f+L_p \le Z \le L \\ EI_p\frac{\partial^4 v}{\partial Z^4}+\frac{\partial}{\partial Z}\left(P(Z)\frac{\partial v}{\partial Z}\right)+\left(\rho_p A_p+M_a\right)\frac{\partial^2 v}{\partial t^2}=Q(Z,t),\ L_f \le Z \le L_f+L_p \end{cases} \tag{12}$$

Called coordinate axis along the length of tower Z, transverse deflection along the Z direction v, axial load $P(Z)$, monopile bending stiffness EI_p, density of the monopile ρ_p, cross-sectional area of the monopile A_p, tower bending stiffness $EI_t(Z)$, density of the tower ρ_t, cross-sectional area of the tower A_t and L_f is length of the monopile, which is located in the seabed. Also, M_a is hydraulic added mass which is calculated by $M_a = C_M \rho_w A_a$ where ρ_w is density of the water and A_a is external area of the monopile. In the aforementioned equations, the first equation is governing differential equation of the platform and the second addresses governing differential equation of the tower. In addition differential equation of the foundations based on the AF model can be presented as follows [46, 50]

$$EI_{f'}\frac{\partial^4 v}{\partial Z^4}+\frac{\partial}{\partial Z}\left(P(Z)\frac{\partial v}{\partial Z}\right)+\left(\rho_{f'}A_{f'}+\mu\right)\frac{\partial^2 v}{\partial t^2}=0,\ 0 \le Z \le L_{f'} \tag{13}$$

where, μ is distributed added mass, $EI_{f'}$ is equivalent bending stiffness, $\rho_{f'}$ is equivalent density and $A_{f'}$ is equivalent cross-sectional area in AF model. Also, differential equation of the foundations according to the DS model is presented as follows [46, 50]

$$EI_f \frac{\partial^4 v}{\partial Z^4} + \frac{\partial}{\partial Z}\left(P(Z)\frac{\partial v}{\partial Z} \right) + K(Z)\cdot v + \rho_f A_f \frac{\partial^2 v}{\partial t^2} = 0,\ 0 \le Z \le L_f \tag{14}$$

where, $K(Z)$ is distributed equivalent stiffness of foundation, ρ_f is foundation density and A_f is cross-sectional area in DS model.

5 APPLYING THE TRANSFER MATRIX METHOD

5.1 Solving the equations of motion

For modeling by the transfer matrix method, the wind turbine structure is discretized into n cylindrical continuous beam elements with constant cross-section as shown in Fig. 5 and the equation of motion is derived for each element. In this case, the axial force, bending stiffness and the cross section for each element take into account constant and differential equation of motion for each element of tower is transformed from the first equation of Eq. (12) as:

$$EI_t \frac{\partial^4 v}{\partial z^4} + P\frac{\partial^2 v}{\partial z^2} + \rho_t A_t \frac{\partial^2 v}{\partial t^2} = 0,\ 0 \le z \le l \tag{15}$$

where l is length of the element and z is element local coordinate along the length of the element as shown in Fig.6. Applying the separation of variables method gives dimensional solution of Eq. (15) for each element of tower as:

$$v(z) = C_1 \cosh s_1 z + C_2 \sinh s_1 z + C_3 \cos s_2 z + C_4 \sin s_2 z \tag{16}$$

where the constant parameters s_1 and s_2 are addressed in Appendix A.

In the same way, differential equation of motion for each of the elements of platform is transformed from the second equation of Eq. (12) as follows

$$EI_p \frac{\partial^4 v(z,t)}{\partial z^4} + P\frac{\partial^2 v(z,t)}{\partial z^2} + \rho_p A_p \frac{\partial^2 v(z,t)}{\partial t^2} = q_i \sin(\omega t) + q_D\left[\cos(\omega t)\cdot\left|\cos\omega t\right|\right],\ 0 \le z \le l \tag{17}$$

In order to apply the TMM, the part $\cos(\omega t)\cdot\left|\cos\omega t\right|$ in Eq. (17) should be expanded into the Fourier's series as:

$$\left|\cos\omega t\right|\cos\omega t = \frac{8}{3\pi}\cos\omega t + \frac{8}{15\pi}\cos 3\omega t - \frac{8}{105\pi}\cos 5\omega t + \frac{8}{315\pi}\cos 7\omega t - \frac{8}{693\pi}\cos 9\omega t + \ldots \tag{18}$$

Substituting of Eq. (18) into Eq. (17), solution of Eq. (17) can be given as:

$$v(z,t) = v(z)\left[q_i \sin\omega t + q_D \sum_{i=1}^{N} A_i \cos a_i \omega t \right] \tag{19}$$

where, N is number of terms in Fourier's series and A_i is Fourier's coefficient. Furthermore, dimensional solution of Eq. (19) for each element can be expressed as:

$$v(z) = C_1 \cosh s_1 z + C_2 \sinh s_1 z + C_3 \cos s_2 z + C_4 \sin s_2 z - (1/\rho_p A_p \omega^2) \tag{20}$$

Solution of foundation elements in AF model is similar to Eq. (16) (see Appendix A). Using the TMM, differential equation of motion for each element of foundation in DS model is transformed from Eq. (14) as:

$$EI_f \frac{\partial^4 v}{\partial z^4} + P\frac{\partial^2 v}{\partial z^2} + K \cdot v + \rho_f A_f \frac{\partial^2 v}{\partial t^2} = 0,\ 0 \le z \le l \tag{21}$$

Eigen values of Eq. (21) can be represented as follows

$$s_1^2, s_2^2 = -\frac{P}{2EI_f} \pm \left(\frac{P^2}{\left(4EI_f\right)^2} - \frac{K - \rho_f A_f \omega^2}{EI_f} \right)^{1/2} \tag{22}$$

Eq. (21) adopts three different solution forms depending on the value of parameters which can be concluded as: while $\omega > \sqrt{K/\rho_f A_f}$ is greater than the cut-on frequency and solution of Eq. (21) is similar to Eq. (15). $\omega = \sqrt{K/\rho_f A_f}$ is the cut-off frequency and $\omega < \sqrt{K/\rho_f A_f}$ is the below the cut off frequency and Eq. (21) has a different solution form [51,52]. In offshore wind turbine tower foundation, value of the K is very large and the excitation frequency of the wave is between 0.20 to 0.25 Hz [46]. Consequently, the excitation frequency is the below the cut off frequency and dimensional solution of Eq. (22) can be expressed as:

$$v(z) = C_1 \cosh az \cos bz + C_2 \cosh az \sin bz + C_3 \sinh az \cos bz + C_4 \sinh az \sin bz \tag{23}$$

where, a and b are given in Appendix A.

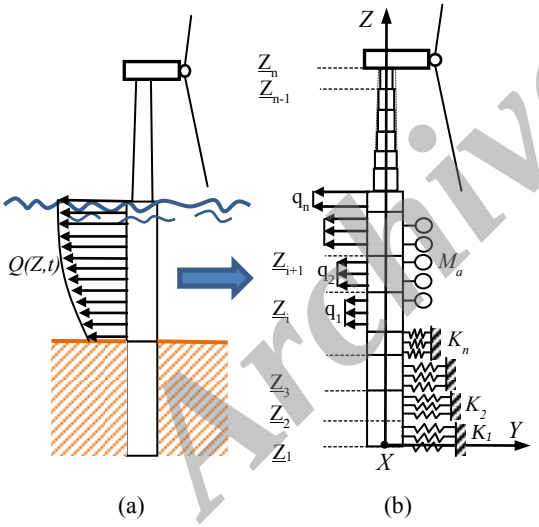

Fig.5
a) Wind turbine towers subjected to the wave force, b) Discretization during applying the TMM.

5.2 Obtaining the transfer matrix

Concluding from the derivation of dimensional solution, the slope θ, shear force V and moment M for each segment are following

$$\begin{aligned} v &= t_{11}C_1 + t_{12}C_2 + t_{13}C_3 + t_{14}C_4 + t_{15} \\ \theta &= \partial v/\partial z = t_{21}C_1 + t_{22}C_2 + t_{23}C_3 + t_{24}C_4 \\ M &= Pv + EI\left(\partial^2 v/\partial z^2\right) = t_{31}C_1 + t_{32}C_2 + t_{33}C_3 + t_{34}C_4 \\ V &= \partial M/\partial z = t_{41}C_1 + t_{42}C_2 + t_{43}C_3 + t_{44}C_4 \end{aligned} \tag{24}$$

where the t_{ij} coefficients are given in the Appendix B. The relations in Eq. (24) can be represented in matrix form as:

$$\begin{bmatrix} v \\ \theta \\ M \\ V \\ 1 \end{bmatrix} = \begin{bmatrix} t_{11} & t_{12} & t_{13} & t_{14} & t_{15} \\ t_{21} & t_{22} & t_{23} & t_{24} & 0 \\ t_{31} & t_{32} & t_{33} & t_{34} & 0 \\ t_{41} & t_{42} & t_{43} & t_{44} & 0 \\ 0 & 0 & 0 & 0 & 1 \end{bmatrix} \begin{bmatrix} C_1 \\ C_2 \\ C_3 \\ C_4 \\ 1 \end{bmatrix} \tag{25}$$

The above equation can be addressed as follows

$$\underline{Z}(z) = T(z).\underline{C} \tag{26}$$

where $\underline{Z(z)}$ is state vector, $\underline{C}$ represents vector of constants and $T(z)$ is called transfer matrix function. By using the TMM, state vector between two nodes i and i-1 shown in Fig. 6 is obtained as follows [53]

$$\underline{Z}_i = T(l)T(0)^{-1}.\underline{Z}_{i-1} = [H]_i.\underline{Z}_{i-1} \tag{27}$$

Herein, $[H]_i$ is transfer matrix between two nodes i and i-1.

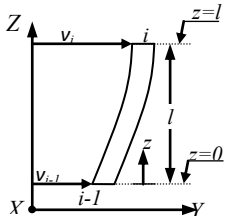

Fig.6
*i*th Element and connected nodes.

In order to apply the TMM on the bottom of tower and elastic base, point matrix can be introduced. In Fig. 7(b), element attached to the nacelle mass is shown. It can be written from the dynamic equilibrium equations

$$\begin{aligned} v_n^t &= v_n^b \\ \theta_n^t &= \theta_n^b \\ M_n^t &= -J\omega^2\theta_n^b + M_n^b \\ V_n^t &= V_n^b + m\omega^2 v_n^b \end{aligned} \tag{28}$$

where, t superscript denotes the top of the element, b superscript denotes the bottom of the element, m is the mass of the nacelle and J is nacelle moment of inertia. Rewriting Eq. (28) in matrix form, the point matrix for concentrated mass at the bottom of the tower is obtained as follows

$$U_{p,n} = \begin{bmatrix} 1 & 0 & 0 & 0 & 0 \\ 0 & 1 & 0 & 0 & 0 \\ 0 & -J\omega^2 & 1 & 0 & 0 \\ m\omega^2 & 0 & 0 & 1 & 0 \\ 0 & 0 & 0 & 0 & 1 \end{bmatrix} \tag{29}$$

In Fig. 7(a), element attached to the CS elastic foundation is shown. Similarly, using the equilibrium equations, the point matrix is obtained can be written as:

$$U_{p,1}=\begin{bmatrix} 1 & 0 & 0 & 0 & 0 \\ 0 & 1 & 0 & 0 & 0 \\ k_{\theta,F} & k_{\theta,M} & 1 & 0 & 0 \\ -k_{u,F} & -k_{u,M} & 0 & 1 & 0 \\ 0 & 0 & 0 & 0 & 1 \end{bmatrix} \tag{30}$$

The state vector is identical for the common elements [53]. Therefore, the state vector between the bottom of the tower and top of the tower in DS and AF foundation models is obtained as follows

$$\underline{Z}_n = U_{p,n}\left[H\right]_{t,n}\left[H\right]_{t,n-1}....\left[H\right]_{t,1}\left[H\right]_{p,n}\left[H\right]_{p,n-1}\cdots\left[H\right]_{p,1}\left[H\right]_{f,n}\left[H\right]_{f,n-1}....\left[H\right]_{f,1}\underline{Z}_1 = \left[H\right]_t\underline{Z}_1 \tag{31}$$

where, $[H]_t$ is total transfer matrix and is obtained by multiplying all the matrices $\left[H\right]_{t,n}$ which each one is the transfer matrix of the *n*th tower segment, $\left[H\right]_{p,n}$ is the transfer matrix of the *n*th monopile segment and $\left[H\right]_{f,n}$ is the transfer matrix of the *n*th foundation segment.

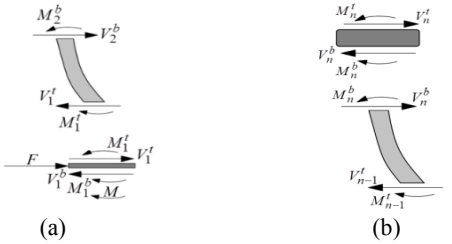

(a) (b)

Fig.7
a) Elements connected to the support in the CS model, b) Elements connected to the nacelle.

Moreover, for the CS foundation model, the State vector between the bottom of the tower and top of the tower is taken as follows

$$\underline{Z}_n = U_{p,n}\left[H\right]_{t,n}\left[H\right]_{t,n-1}....\left[H\right]_{t,1}\left[H\right]_{p,n}\left[H\right]_{p,n-1}\cdots\left[H\right]_{p,1}U_{p,1}\underline{Z}_1 = \left[H\right]_t\underline{Z}_1 \tag{32}$$

5.3 Applying boundary conditions

For all three foundation models including the DS, AF and CS, the value of $V_n{}^t$ and $M_n{}^t$ are equal to zero at the end of the tower besides in the AF model fulcrum is clamped. Therefore, the slope and displacement at the base of the tower keep being zero for the AF model and the state vector between the 1th segment and the *n*th segment is obtained as follows, correspondingly

$$\begin{bmatrix} v \\ \theta \\ 0 \\ 0 \\ 1 \end{bmatrix}_n = \begin{bmatrix} a_{11} & a_{12} & a_{13} & a_{14} & a_{15} \\ a_{21} & a_{22} & a_{23} & a_{24} & a_{25} \\ a_{31} & a_{32} & a_{33} & a_{34} & a_{35} \\ a_{41} & a_{42} & a_{43} & a_{44} & a_{45} \\ 0 & 0 & 0 & 0 & 1 \end{bmatrix}\begin{bmatrix} 0 \\ 0 \\ M \\ V \\ 1 \end{bmatrix}_1 \tag{33}$$

Using the above equation, bending moment and shear force on the first segment, and displacement and slope at the end segment are obtained as follows

$$\begin{bmatrix} M_1 \\ V_1 \\ v_n \\ \theta_n \end{bmatrix} = \begin{bmatrix} a_{13} & a_{14} & -1 & 0 \\ a_{23} & a_{24} & 0 & -1 \\ a_{33} & a_{34} & 0 & 0 \\ a_{43} & a_{44} & 0 & 0 \end{bmatrix}^{-1}\begin{bmatrix} -a_{15} \\ -a_{25} \\ -a_{35} \\ -a_{45} \end{bmatrix} \tag{34}$$

In DS and CS models, fulcrum is free. Therefore, the bending moment and shear force at the base of the tower are taken to be zero and the state vector between the 1th segment and the *n*th segment can be obtained as follows, correspondingly

$$\begin{bmatrix} v \\ \theta \\ 0 \\ 0 \\ 1 \end{bmatrix}_n = \begin{bmatrix} a_{11} & a_{12} & a_{13} & a_{14} & a_{15} \\ a_{21} & a_{22} & a_{23} & a_{24} & a_{25} \\ a_{31} & a_{32} & a_{33} & a_{34} & a_{35} \\ a_{41} & a_{42} & a_{43} & a_{44} & a_{45} \\ 0 & 0 & 0 & 0 & 1 \end{bmatrix} \begin{bmatrix} v \\ \theta \\ 0 \\ 0 \\ 1 \end{bmatrix}_1 \tag{35}$$

In a same manner to the previous case, the displacement and slope at the beginning and end of the tower for the DS and CS models can be obtained as follows

$$\begin{bmatrix} v_1 \\ \theta_1 \\ v_n \\ \theta_n \end{bmatrix} = \begin{bmatrix} a_{11} & a_{12} & -1 & 0 \\ a_{21} & a_{22} & 0 & -1 \\ a_{31} & a_{32} & 0 & 0 \\ a_{41} & a_{42} & 0 & 0 \end{bmatrix}^{-1} \begin{bmatrix} -a_{15} \\ -a_{25} \\ -a_{35} \\ -a_{45} \end{bmatrix} \tag{36}$$

6 RESULTS AND DISCUSSION

In order to examine the accuracy of the proposed method, response of the 5-MW wind turbine tower subjected to the wave excitation force is evaluated using the TMM and the results are compared with the FEM analyzed based data [54]. In [36], dimensions and materials used in wind turbine towers are presented. Table 2. shows the characteristics of the foundation in the CS and AF models [55]. Table 3. describes the parameters required to identify the wave force [54]. Schematic of soil installation, corresponding physical properties and stiffness of tower foundation for the DS model are shown in Fig. 8 [46].

Table 2
Profile foundation in AF and CS models. [55]

Characteristics	Value
Equivalent stiffness_ $k_{u,F}$ (N.m^{-1})	2.58×10^{9}
Equivalent stiffness_ $k_{u,M}$ (N.rad^{-1})	-2.26×10^{10}
Equivalent stiffness_ $k_{\vartheta,F}$ (N.m.m^{-1})	-2.26×10^{10}
Equivalent stiffness_ $k_{\vartheta,M}$ (N.m.rad^{-1})	2.64×10^{11}
Equivalent high in AF model (m)	17.5
Equivalent diameter in AF model (m)	6.2132
Equivalent thickness in AF model (m)	0.05986

Table 3
Required parameters to identify the wave force. [54]

Characteristics	Value
Mass coefficient	2
Density (Kg.m^{-3})	1000
Wave height (m)	6
Water depth (m)	20
Wave length (m)	58
Wave period (sec)	10
Drag coefficient	1

Fig.8
a) Soil physical properties, b) Stiffness of the foundation for the DS model.[46]

To determine the transfer matrix for each element and obtain the response of the wind turbine tower under the wave load, the wind turbine tower is discretized in MATLAB software. For this purpose, two concerns should be investigated, first, the number of terms in the Fourier's series could be sufficiently accurate and the second, the number of elements in modeling of wind turbine towers could be provided with adequate accuracy. It is well-known that when the number of elements and also the number of included Fourier's coefficients are increased, the model would be closer to the realistic model and so the accuracy of the results increases however the volume of calculations is proportional to theses increasing. Thus the number of elements and the number of Fourier's terms should be chosen in such a way that they benefit from high accuracy and low volume of calculations time as possible. In order to estimate the suitable number of terms in the Fourier's series, 100 elements for wind turbine towers are considered as default and displacement time history of the tower tip depicts for models DS, AF and CS extracted by the TMM in Figs. 9 to 11. Curves in the figures are corresponding to the one to five first Fourier's expansion terms. As it is clear from the figures, after the three first terms, time history diagrams are overlapped. So it can be concluded that taking into account the three first terms in Fourier's series for each of the three foundation models is reasonably accurate. For a closer look at this issue and determining the amount of error for use of the included terms in Fourier's series, the difference results in using the terms number are presented in Figs. 12(a) to 12(d). To this end, difference between the two considered terms and the one considered term in Fig. 12(a), difference between the three included terms and the two included terms in Fig. 12(b), difference between the four and three terms in Fig. 12(c) and difference between the considered five and four terms in Fig. 12(d) are shown. As can be seen from the above figures, taking just one term of the Fourier's series leads to the maximum error 1.5×10^{-2} *m*, considering two terms, maximum error is equal to 1.9×10^{-3} *m*, by including three terms, maximum error 7×10^{-4} *m* is given and finally by taking four terms, maximum error is evaluated as 2.9×10^{-5} *m*. So containing the three terms of the Fourier's series, error order will be in order of ten thousandths. Thus in what follows; the three first terms of the Fourier's series expansion are considered to address the results of analysis, accordingly. It should be noted that the use of the first three terms cannot be generalized to all relevant systems. So accuracy requirement about the number of included terms must be examined for each problem individually. It is possible that more number of included terms would be necessary for an accurate convergence in other case studies.

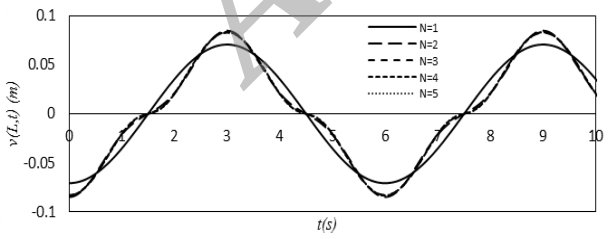

Fig.9
Deflection time history of the tower tip for the one to five first Fourier's series terms in the DS model.

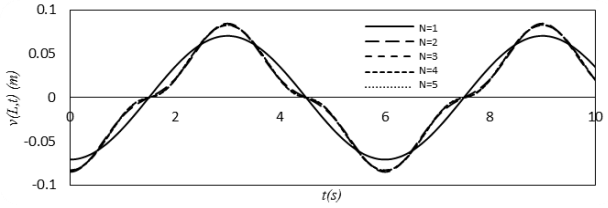

Fig.10
Deflection time history of the tower tip for the one to five first Fourier's series terms in the AF model.

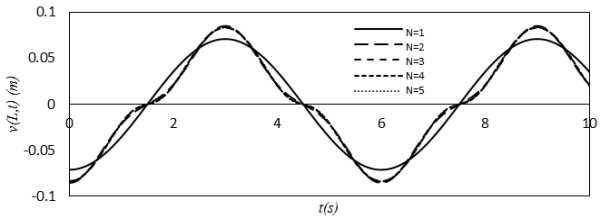

Fig.11
Deflection time history of the tower tip for the one to five first Fourier's series terms in the CS model.

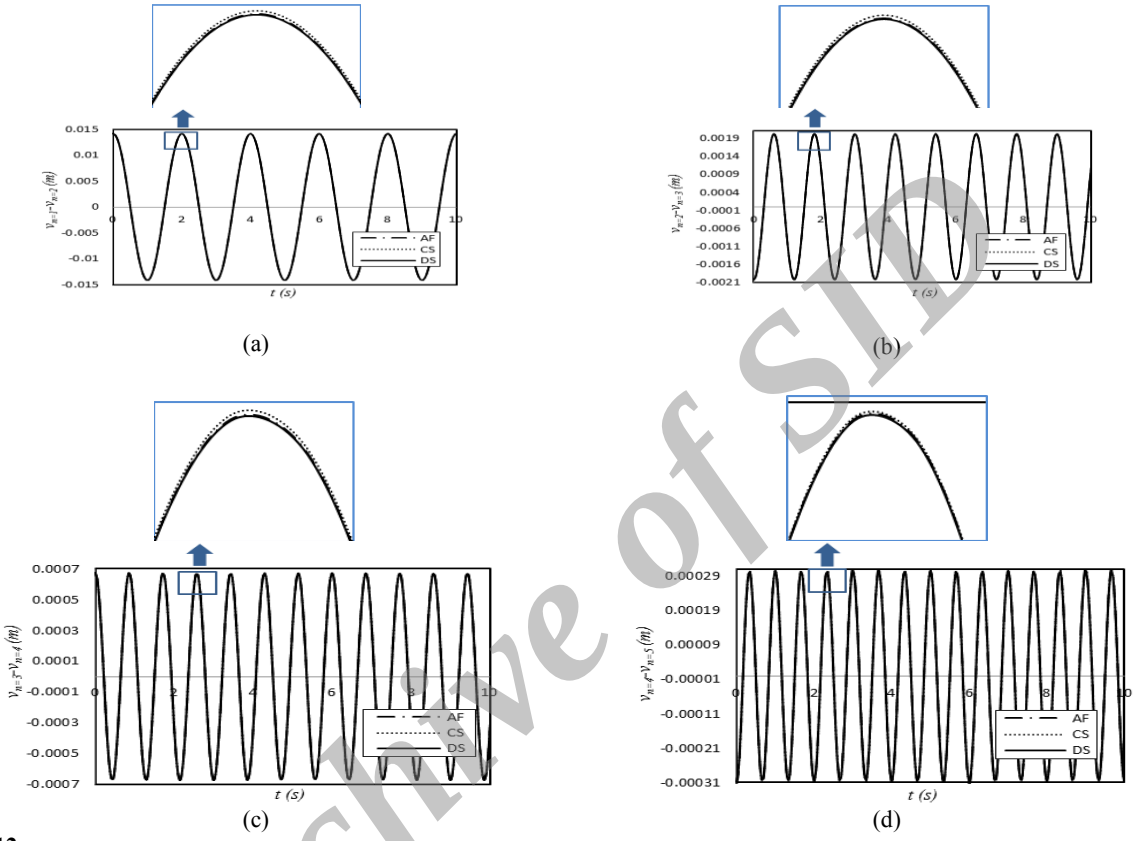

Fig. 12
Variation of results in employing of the number of Fourier's series terms, a) Difference between employing 2 terms and 1 term, b) Difference between 3 included terms and 2 terms, c) Difference between 4 and 3 considered terms d) Difference between 5 and 4 included terms.

The next issue that must be addressed is the number of tower elements. For this purpose, the number of elements in accordance with the desired accuracy and volume of calculations is examined. Table 4. shows the hardware and software specifications of personal computer employed for the analysis and the results are shown in Table 5. In the abovementioned table, the maximum numerical error for different number of elements and the corresponding MATLAB simulation time is displayed. It can be addressed from the table the error decreases monotonically with increasing number of elements and in front, the time consumed computations can be increased for the three foundation types. Therefore, by selecting 9 elements for AF and DS models, including 5 elements for tower, 2 elements for monopile and 2 elements for foundation and also 5 elements for CS model including 5 elements for tower and 2 elements for monopole, maximum error approaches to 8.53×10^{-2} *m*. With increasing number of elements to 25 elements for the AF and DS models and to 20 elements for CS model maximum error equals to 1.4×10^{-2} *m* and as a last mesh sensitivity, by selection of 80 elements for AF and DS models and selecting the 60 elements for CS model, the maximum error is less than 5×10^{-2} *m* Therefore, selection of 80 elements for AF and DS models and selection 60 elements for CS model can be accurate and so the this number of elements is considered for the later analyzes. Also by examining the simulation time in MATLAB, it gives that among the three foundation models, the DS model takes the longest simulation time and the shortest simulation time belongs to CS model. Due to this finding, the transfer matrix model of the DS model is more complex than the CS and AF models. On the other

hand, the CS model includes no foundation at the base that this fact provides fewer elements than CS and AF model. Thus, the corresponding simulation time in the CS model is less than the AF model, naturally.

Table 4
Hardware and software specifications of the used personal computer.

Item	Value
OS Name	Microsoft Windows 7 Ultimate
System Model	HP ProBook 4520s
Processor	Intel(R) Core(TM) i5 CPU M 480 @ 2.67GHz
Installed Physical Memory (RAM)	4.00 GB
Version	6.1.7601 Service Pack 1 Build 76016
System Type	X86-based PC
Hardware Abstraction Layer	Version = "6.1.7601.17514"
Available Virtual Memory	4.29 GB

Table 5
Maximum error for a number of different elements and corresponding MATLAB simulation time.

Model	Number of Elements			The maximum error between the number of elements	Simulation time in MATLAB (second)
	tower	monopile	foundation		
DS	5	2	2	……	1.1200075
	10	10	5	0.085300150	1.1691306
	15	15	10	0.014739865	1.2687001
	20	20	15	0.002696329	1.3572087
	30	30	20	0.000499832	1.4352092
	40	40	25	0.000175063	1.5288098
	50	50	30	0.000081081	1.6536106
AF	5	2	2	……	0.7800050
	10	10	5	0.085245688	0.9372062
	15	15	10	0.014592466	1.0865701
	20	20	20	0.002694727	1.1612077
	30	30	30	0.000499532	1.2460085
	40	40	40	0.000174957	1.3168103
	50	50	50	0.000081030	1.4340115
CS	5	2	…	……	0.7644049
	10	10	…	0.085215634	0.8736055
	15	15	…	0.014582340	0.9012504
	20	20	…	0.002693944	0.9516060
	30	30	…	0.000499380	1.0296066
	40	40	…	0.000174901	1.1388072
	50	50	…	0.000081003	1.2948083

In the following, corresponding results of the three abovementioned foundation models are discussed to compare the support effects. For this purpose, Response of the drag force and response of the inertia force on the tower is presented in Figs. 13, 14, respectively. Each of the figures contains diagrams showing the effects of all three foundation models DS, AF and CS on the results. At the right hand side of the figures, the maximum amplitude of each diagram is magnified to compare the results of each foundation models. The magnification reveals that for both drag and inertia force, CS model takes the highest tower tip deflection and DS model has the smallest tower tip deflection. As shown in the right side schemes, the difference between AF and DS models results are minimal and the corresponding responses are roughly consistent. Consequently, it can be concluded, applying the CS model leads to additional approximation with respect to the DS model in the results.

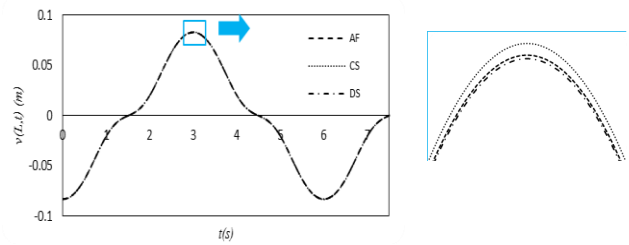

Fig.13
Response of the drag force for all three foundation models DS, AF and CS by taking into account the three first Fourier's series terms.

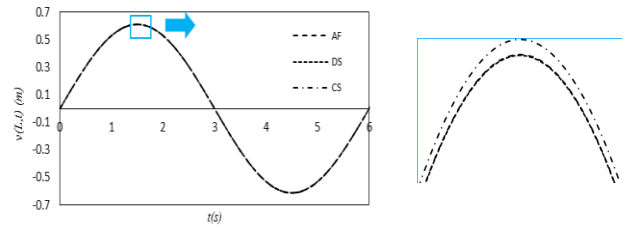

Fig.14
Response of the inertia force for all three foundation models DS, AF and CS in which three first Fourier's series terms taken into account.

Fig. 15 shows response of the wind turbine tower by virtue of the drag force, inertia force and total wave force for DS foundation model. As it is clear from the figure, the maximum displacement of the tower tip is due to the inertia force and small amount of displacement is caused by the drag force whereas, maximum displacement of the inertial force is 0.6 m and maximum displacement of the drag force is 0.07 m. This fact is raised from the squared wavelength (λ^2) in the denominator of the inertial force relation while the amount of wavelength is much larger. Thus, the drag force contributes as a small part of the wave force. To clarify this interesting finding, the distribution of inertia and drag forces amplitude upon the platform height is reported in Figs. 16(a) and 16(b), respectively. As can be concluded from the figure, Maximum drag and inertia forces occur on the water surface and the corresponding numerical values are 69099 N and 16520 N, respectively. The data imply maximum inertia force is more than twice of maximum drag force. On the other hand, inertia force induced maximum displacement is eight times the drag maximum displacement due to drag force roughly. This outcome is because of the variations of Inertia and drag force along the platform. Comparing figures 16a and 16b, presents drag force variations is much greater than the inertial force variations by increasing the depth whereas at the depth of 19 m, the inertial and drag forces are equal to 39078 and 3855 N respectively. This result suggests that drag force is reduced up to 94% whereas inertia force is declined to 75%. Consequently, the maximum displacement of the tower is contributed by the inertia force.

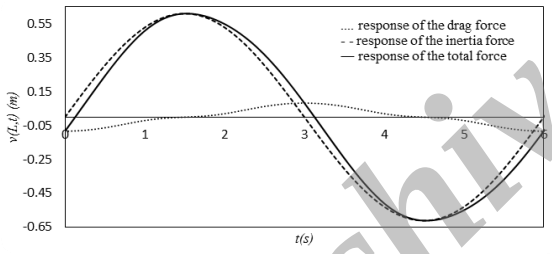

Fig.15
Response of the inertia force, drag force and total force for DS foundation model.

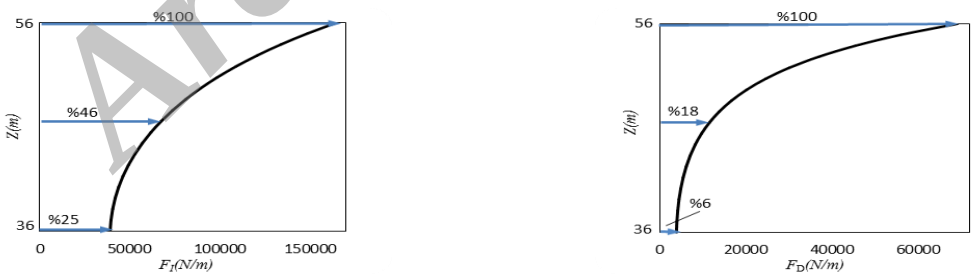

(a) (b)

Fig.16
Amplitude of the drag and inertia force upon the monopile height, a) Inertia force, b) Drag force.

In the following, numerical comparison between the results of transfer matrix method and finite element method [54] is examined. In [54] dynamic response of the wind turbine tower under Morrison wave force by Airy's theory has been predicted using the finite element method. The DS foundation model has been included in the analysis [54]. For this purpose, the wind turbine tower divided into 1001 cylindrical elements including 609 elements for tower, 140 elements for monopile and 252 elements for foundation in Fast software. For easier modeling in Fast, the

authors of [54] have used 252 linear springs on the desired discrete point of the foundation instead of distributed spring. In addition, a concentrated force has been applied on each element to model the axial force which led to increasing the number of elements in [54]. However in the presented paper, differential equation of motion for each element is solved analytically. Therefore, fewer numbers of elements is used. For this purpose, the wind turbine tower is divided into 106 elements including 50 elements for tower, 20 elements for monopile and 36 elements for foundation. Distributed spring is used for foundation elements and axial force per unit length is considered for all elements.

Figs. 17 and 18 address time history of bending moment and shear force at the support platform for both of the presented TMM and FEM analysis provided in [8]. By observing the figures, it can be seen that for the bending moment in Fig. 17, little difference can be reported between the results of the TMM and the FEM. For the shear force comparison in Fig. 18 the difference is reasonably a little more. This fact comes from that the shear force includes the higher order of derivation than the bending moment. As it is well-known, the shear force is obtained from the third derivative of deflection whereas the bending moment is gained from the second derivative of deflection function. So, the relative difference in shear force is obviously greater than bending moment. It can be concluded from the figures that the TMM result is in good agreement with the results of finite element method in spite of low computational cost.

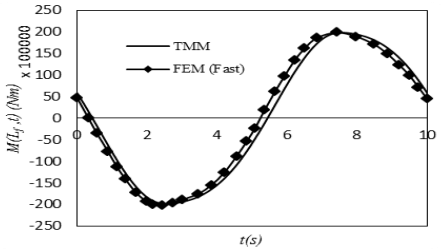

Fig.17
Comparison of the TMM results with the FEM result [54] about the bending moment time history at the support platform.

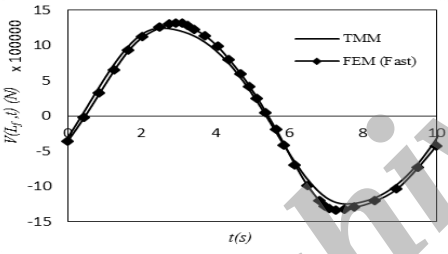

Fig.18
Comparison of the TMM results with the FEM result [54] about the shear force time history at the support platform.

Of a particular interest, one can observe the influence of the wave force parameters on the dynamic response of the tower. For this purpose, the effect of water depth change on the dynamic displacement of the tower tip in several mass coefficients is examined in Fig. 19 using the presented analysis. As can be seen from the figure, at all coefficients, increasing water depth leads to decrease the maximum tower deflection. On the other hand, the slope of the v-d_w diagram declines by increasing water depth whereas the slope approaches close to zero at the depth of 20 m. The effect of changes in water depth on the maximum dynamic deflection of wind turbine towers can be observed from the term $\psi=\cosh[2\pi(\zeta+d_w)/\lambda]/\cosh(2\pi d_w/\lambda)$ exists in the wave force relation Eq. (5). Considering that the coordinate parameter ζ adopts a negative value in aforementioned definition for ψ, thus the fraction ψ would take an amount smaller than the unit by increasing d_w. Consequently, the wave force amplitude would also be decreased by increasing in d_w. This result can be elucidated by diagram depicted in Fig. 21 which shows the variations of the function ψ in terms of water depth d_w and parameter ζ. It can be clearly seen from the figure that at all values of ζ, function ψ will be decreased by increasing in d_w and therefore reducing the function ψ leads to declining wave force amplitude and the maximum dynamic deflection of tower decreased subsequently. For clarifying the application of this finding, assume two wind turbines with the same dimensions installed in a wind farm. One of the turbines is installed at a depth of 10 meters and another is installed at the 18 m depth and the added mass coefficient is 1.5 for both of them. When the water level rises 2 meters, using Fig. 19, one can obtain the maximum dynamic displacement of the turbine installed at a depth of 10 m reaches from 0.81 m to 0.67 m and the maximum dynamic displacement of the turbine installed at a depth of 18 m reaches from 0.51 m to 0.48 m, too. Thus, since the tide occurs twice a day, so the wind turbine is subjected to stress changes twice a day correspondingly. Consequently it can be concluded that in a wind farm, tidally water depth changes have little effect on the dynamic response of

turbines installed in more depth and merely change of mass coefficient is effective on their dynamic response. On the other hand, the dynamic response of turbines installed in less depth changes significantly during the tide and water depth changes and this matter should be taken into consideration in their fatigue analysis and design.

As another parametric study to achieve meaningful result, in Fig. 20, the effect of wave height variations on the tower tip deflection in a number of mass coefficients is investigated. As the figure reports, the tower displacement possesses a linear proportional relationship with wave height. Moreover, increasing mass coefficient goes to enlarge the maximum displacement. Consequently, whereas surface roughness of offshore wind turbine platforms intensify during long time operation of the platforms subsequently the maximum tower deflection would increase and also stress on the wind turbine platforms would be critical accordingly.

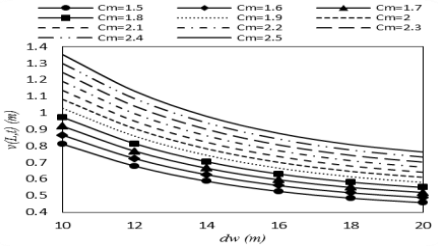

Fig.19
Effect of water depth on the dynamic tower deflection in various mass coefficient (H=10m, T=6s).

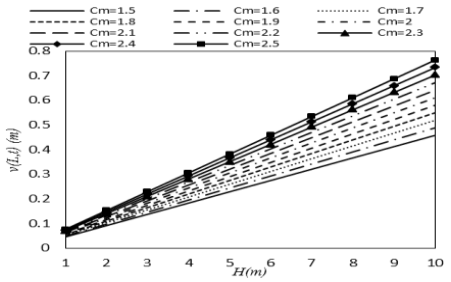

Fig.20
Effect of wave height variations on the tower deflection in various mass coefficient (T=6s).

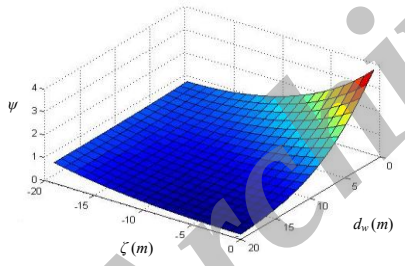

Fig.21
Variation of function ψ versus water depth d_w and coordinate parameter ζ.

As a case study to present applicable and significant outcome, the frequency response of the wind turbine tower for climate of the Persian Gulf is examined. Wave height varies in different parts of the Persian Gulf and it can be evaluated from 0.5 to 4 m. However, at the most areas, wave height is approximately 1.6 m [43]. According to previous studies, time interval between waves in the northern part of the Persian Gulf is approximately 3 to 5 seconds and in the southern parts is reported a little more [43].

5-MW wind turbine geometry mentioned in the previous sections 15 m water depth is adopted for the analysis as well the rotor angular velocity is considered in the range of 7 to 12 rpm (0.12 to 0.2 Hz). Fig. 22 shows the maximum dynamic response of the tower to wave height between 0.5 to 3 m. Moreover, 1P and 3P frequency regions are depicted in the figure, according to the range of rotor angular velocity. As can be seen from the diagram, wave frequency range is not laid between the excitation frequency range (1P and 3P). Therefore, selecting the rotation range among the 7 to 12 rpm is practical and efficient. Nevertheless, the first natural frequency is located within the wave frequency range which leads to resonance and catastrophic failure of the whole structure finally. In consequence, the frequency region selected for the wind farm installation should be far from the natural frequencies and the range of excitation frequencies. By observing, the appropriate frequency range and corresponding response can be found in Fig. 22. As shown in the figure, frequency range from 1.7 to 2.1 radians per second is suitable for installation the wind farm. Therefore, by examining the different parts of the Persian Gulf, region must be chosen

where the wave frequency range from 1.7 to 2.1 radians per second does not exceed. Somewhere is the best area where the rotation frequency is closer of the 1.2 radians per second.

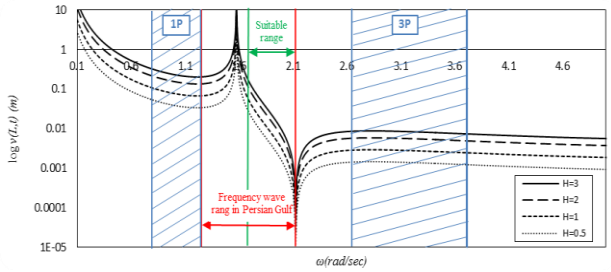

Fig.22
Frequency response of the tower to wave height between 0.5 to 3 *m*.

In order to confirm the transfer matrix method results, another case study is discussed in this section and TMM results is compared with experimental data for a 3 MW offshore wind turbine presented in [56]. In [56] natural frequencies of the wind turbine tower were calculated by installing four accelerometer sensors and using signal analysis software. Characteristics of dimensions of the 3 MW offshore wind turbine are listed in [57]. To evaluate the importance of foundation modeling, natural frequency of the tower in two modes, one with respect to a fixed fulcrum for the tower and the other using the elastic foundation model is calculated. Due to the lack of information on soil physical properties and the forces acting on the tower, the CS foundation model is applied. For this purpose, the wind turbine tower is divided into 80 elements and the frequency response under external force is predicted. Finally, natural frequencies of the wind turbine tower can be reported using the bounce points in frequency response. The results are shown in Table 6. As it is clear from the table, TMM relative error on the first natural frequency evaluates about 2% and relative error can be estimated approximately 10% on the second natural frequency for the CS foundation model. This is while relative error can be reported about 9% in the first mode and about 35% in the second mode for fixed fulcrum model. This examination indicates that the modeling of wind turbine foundation is very significant and the error in the results can be increased dramatically using a fixed fulcrum model. On the other hand, this study demonstrates the accuracy of the transfer matrix method assuming the CS model which presents the relative error will be less than 2% for the first natural frequency and less than 10% for the second natural frequency.

Table 6
Comparison between the transfer matrix method results and experimental data. [56]

Number of Mode	Transfer matrix method with CS model		Transfer matrix method with fixed fulcrum model		Experimental data (Hz)
	Natural frequency (Hz)	Relative error (%)	Natural frequency (Hz)	Relative error (%)	
First mode	0.3546	1.77	0.3927	8.80	0.3610
second mode	1.7052	9.30	2.1080	35.12	1.5600

7 CONCLUSIONS

In this paper, an analytical method for predicting the steady response of the offshore wind turbine tower with fixed monopile platform under Morrison wave force was presented. For this purpose, initially, three models were introduced for the tower foundation. Speculating the scope and scale of the tower, the Euler-Bernoulli's beam differential equation was used to state the transfer matrix for each element of the tower, platform and foundation. Then, by applying the relevant boundary conditions along with constructing the point matrix, the required equation for determination of wind turbine tower response is obtained. Finally, the procedure achieved by the presented transfer matrix method are applied in several case studies that results can be categorized as follows

1. If information about the physical installation is available, DS and AF models can be used accurately and the DS model is more accurate than the other models although the simulation time increases slightly compared to the CS and AF models. On the other hand, CS model is less accurate than the DS and AF models and can be used when detailed information is not available for soil installation.
2. In all mass coefficients, increasing water depth gives rise to reduce the maximum displacement of wind turbine tower and this matter is more important for turbines installed in more depth. Thus in a wind farm,

stress amplitude of turbines installed in less depth includes greater changes. This concern should be considered in their fatigue analysis and design.

3. Transfer matrix method result is in good agreement with the results of finite element method and experimental data that this shows the accuracy of the transfer matrix method. Consequently, transfer matrix method can be used as an analytical method with high accuracy in vibration analysis of wind turbine tower under the Morrison wave force by Airy's theory.

APPENDIX A

s_1 and s_2 parameters

By solving the governing differential equations of motion, s_1 and s_2 parameters can be calculated for each of the models.

s_1 and s_2 for the tower elements can be expressed as:

$$s_1^2, s_2^2 = -\frac{P}{2EI_t} \pm \left(\frac{P^2}{\left(2EI_t\right)^2} + \frac{\rho_t A_t \omega^2}{EI_t} \right)^{1/2}$$

Similarly, s_1 and s_2 for the monopile elements can be expressed as:

$$s_1^2, s_2^2 = -\frac{P}{2EI_p} \pm \left(\frac{P^2}{\left(2EI_p\right)} + \frac{\left(\rho_p A_p + M_a\right)\omega^2}{EI_p} \right)^{1/2}$$

Also for the foundation elements in AF model can be expressed as:

$$s_1^2, s_2^2 = -\frac{P}{2EI_{f'}} \pm \left(\frac{P^2}{\left(2EI_{f'}\right)} + \frac{\left(\rho_{f'} A_{f'} + \eta\right)\omega^2}{EI_{f'}} \right)^{1/2}$$

APPENDIX B

t_{ij} coefficients

t_{ij} coefficients for elements of the tower, monopile and foundation in AF model is obtained as follows

$$\begin{array}{llll}
t_{11} = \cosh s_1 z & t_{21} = s_1 \sinh s_1 z & t_{31} = (P + EI_\alpha s_1^2)\cosh s_1 z & t_{41} = (P + EI_\alpha s_1^2) s_1 \sinh s_1 z \\
t_{12} = \sinh s_1 z & t_{22} = s_1 \cosh s_1 z & t_{32} = (P + EI_\alpha s_1^2)\sinh s_1 z & t_{42} = (P + EI_\alpha s_1^2) s_1 \cosh s_1 z \\
t_{13} = \cos s_2 z & t_{23} = -s_2 \sin s_2 z & t_{33} = (P - EI_\alpha s_2^2)\cos s_2 z & t_{43} = -(P - EI_\alpha s_2^2) s_2 \sin s_2 z \\
t_{14} = \sin s_2 z & t_{24} = s_2 \cos s_2 z & t_{34} = (P - EI_\alpha s_2^2)\sin s_2 z & t_{44} = (P - EI_\alpha s_2^2) s_2 \cos s_2 z
\end{array}$$

In the above, bending stiffness is addressed by EI_α in which for tower $\alpha=t$, for monopile $\alpha=p$ and for foundation in AF model $\alpha=f'$. Also, for monopile elements $t_{15} = 1/\rho_p A_p \omega^2$ and for the other elements t_{15} is set to zero.Similarly, for DS foundation model is obtained as follows

$$\begin{array}{lll}
t_{11} = \cosh az \cos bz & t_{23} = at_{11} - bt_{14} & t_{41} = (ra - 2ab^2 EI_f)t_{13} - (rb + 2a^2 bEI_f)t_{12} \\
t_{12} = \cosh az \sin bz & t_{24} = at_{12} + bt_{13} & t_{42} = (ra - 2ab^2 EI_f)t_{14} + (rb + 2a^2 bEI_f)t_{11} \\
t_{13} = \sinh az \cos bz & t_{31} = rt_{11} - 2abEI_f t_{14} & t_{43} = (ra - 2ab^2 EI_f)t_{11} - (rb + 2a^2 bEI_f)t_{14} \\
t_{14} = \sinh az \sin bz & t_{32} = rt_{12} + 2abEI_f t_{13} & t_{44} = (ra - 2ab^2 EI_f)t_{12} + (rb + 2a^2 bEI_f)t_{13} \\
t_{21} = at_{13} - bt_{12} & t_{33} = rt_{13} - 2abEI_f t_{12} & r = P + \left(a^2 - b^2\right)EI_f, \quad a = \left(\sqrt{1-c}\right)d, \quad b = \left(\sqrt{1+c}\right)d \\
t_{22} = at_{13} + bt_{11} & t_{34} = rt_{14} + 2abEI_f t_{11} & c = P \Big/ \sqrt{4EI_f\left(K - \rho_f A_f \omega^2\right)}, \quad d = \left(K - \rho_f A_f \omega^2 / 4EI_f\right)^{0.25}
\end{array}$$

REFERENCES

[1] Herbert G.M., Iniyan S., Sreevalsan E., Rajapandian S., 2007, A review of wind energy technologies, *Renewable and Sustainable Energy* **11**: 1117-1145.

[2] Manwell J.F., McGowan J.G., Rogers J.G., 2002, Wind Energy Explained (Theory, Design and Application), John Wiley & Sons.

[3] Data sheet offshore wind energy, 2010, *European Wind Energy Association*, Publishing Physics Web, www.ewea.com.

[4] Mostafaeipour A., 2010, Feasibility study of offshore wind turbine installation in Iran compared with the world, *Renewable and Sustainable Energy* **14**: 1-22.

[5] Samani M., Zadegan H., Saibani M., 2011, Feasibility study of offshore wind turbine installation in the Persian Gulf, *Proceedings of the 13th Marine Industries Conference* .

[6] Kaljahi A., Lotfollahi M., 2013, Performance analysis of tension leg platform offshore wind turbine in The Caspian Sea, *Proceedings of the First New Energy Conference*.

[7] Kaljahi A., Lotfollahi M., 2013, Technical feasibility study of using offshore wind turbine in the Iran, *Proceedings of the First New Energy Conference*.

[8] Breton S.P., Moe G., 2009, Status, plans and technologies for offshore wind turbines in Europe and North America, *Renewable Energy* **34**: 646-654.

[9] Van Bussel G.J.W., Zaaijer M.B., 2001, Reliability, availability and maintenance aspects of large scale offshore wind farms, *Proceedings of the MAREC*.

[10] Bhattacharya S., Lombardi D., Wood D.M., 2010, Similitude relationships for physical modeling of monopile-supported offshore wind turbines, *International Journal of Physical Modeling in Geotechnics* **11**: 58-68.

[11] Kim K.T., Lee C.W., 2011, Structural vibration analysis of large-scale wind turbines considering periodically time-varying parameters, *Proceedings of the 13th World Congress in Mechanism and Machine Science*.

[12] Chaoyang F., Nan W., Bol Z., Changzheng C., Dynamic performance investigation for large-scale wind turbine tower, *Proceedings of the IEEE***.**

[13] Bazeos N., Hatzigeorgiou G. D., HondrosI D., Karamaneas H., Karabalis D. L., Beskos D. E., 2002, Static, seismic and stability analyses of a prototype wind turbine steel tower, *Engineering Structures* **24**: 1015-1025.

[14] Salehi S., Pirooz M., Daghigh M., 2009, Aerodynamic and structural analysis of offshore wind turbine tower in The Persian Gulf, *Proceedings of the Marine industries conference*.

[15] Lavassas G., Nikolaidis G., Zervas P., Efthimiou E., Doudoumis I.N., Baniotopoulos C.C., 2003, Analysis and design of the prototype of a steel 1-MW wind turbine tower, *Engineering Structures* **25**: 1097-1106.

[16] He Z., Jianyuan X., Xiaoyu W., 2009, The dynamic characteristics numerical simulation of the wind turbine generators tower based on the turbulence model, *Proceedings of the International Conference on Industrial Electronics and Applications*.

[17] Bush E., Manuel L., 2009, Foundation models for offshore wind turbines, *Proceedings of the Aerospace Sciences Meeting Including the New Horizons Forum and Aerospace Exposition*.

[18] Passon P., Kühn1M., Butterfield S., Jonkman J., Camp T., Larsen T.J., 2007, OC3 benchmark exercise of aero-elastic offshore wind turbine codes, *Journal of Physics*, *Conference Series* **75**: 1-12.

[19] Chen J., Jiang D., 2010, Modal analysis of wind turbine tower, *Proceedings of the IEEE*.

[20] Murtagh P.J., Basu B., Broderick B.M., 2004, Simple models for natural frequencies and mode shapes of towers supporting utilities, *Computers and Structures* **84**: 1745-1750.

[21] Maalawi Y., 2007, A Model for yawing dynamic optimization of a wind turbine structure, *International Journal of Mechanical Sciences* **49**: 1130-1138.

[22] Wang J., Qin D., Lim T., 2010, Dynamic analysis of horizontal axis wind turbine by thin-walled beam theory, *Journal of Sound and Vibration* **325**: 3565-3586.

[23] Kort D.A., 2003, The transfer matrix method applied to steel sheet pile walls, *International Journal for Numerical and Analytical Methods in Geomechanics* **27**: 453-472.

[24] Dawson B., Davies M., 1974, An improved transfer matrix procedure, *International Journal for Numerical Methods in Engineering* **8**: 111-117.

[25] Tso W.K., Chan P.C.K., 1973, Static analysis of stepped coupled walls by transfer matrix method, *Building science* **8**: 167-177.

[26] Holzer H., 1921, *Die Berechnung der Drehschwingungen*, Springer.

[27] Myklestad N.O., 1944, New method of calculating natural modes of uncoupled bending vibrations of airplane wings and other types of beams, *Aeronaut Science* **6**: 153-166.

[28] Pestel C., Leckie A., 1963, *Matrix Methods in Elastomechanics*, McGraw Hill, New York.

[29] Dai H.L., Wang L., Qian Q., Gan J., 2012, Vibration analysis of three-dimensional pipes conveying fluid with consideration of steady combined force by transfer matrix method, *Applied Mathematics and Computation* **219**: 2453-2464.

[30] Orasanu N., Craifaleanu A., 2011, Theoretical and experimental analysis of the vibrations of an elastic beam with four concentrated masses, *Proceedings of the SISOM 2011 and Session of the Commission of Acoustics*.

[31] Li Q.S., Fang J.Q., Jeary A.P., 2000, Free vibration analysis of cantilevered tall structures under various axial loads, *Engineering Structures* **22**: 525-534.

[32] Rohani A., 2002, Vibration analysis of rotor, bearing and membrane system in a Gas turbine, *Msc Thesis, Sharif University of Technology*,Tehran.
[33] Uhrig R., 1966, The transfer matrix method seen as one method of structural analysis among others, *Journal of Sound and Vibration* **4**: 136-148.
[34] Fallah A., 1999, Lateral vibration analysis of ship's rotor, *Msc Thesis, Sharif University of Technology*, Tehran.
[35] Farshidianfar A., Hoseinzadeh M., Raghebi M., 2008, A novel way for crack detection in rotors using mode shape changes, *Journal of Mechanic and Aerospace* **8**: 23-37.
[36] Bababake M., 2004, Vibration analysis of rotor-bearing system by transfer matrix method, *Msc Thesis, Sharif University of Technology*, Tehran.
[37] Meng W., Zhangqi W., Huaibi Z., 2009, Analysis of wind turbine steel tower by transfer matrix method, *Proceedings of the International Conference on Electrical Engineering*.
[38] Meng W., Zhangqi W., 2011, The vibration frequencies of wind turbine steel tower by transfer matrix method, *Proceedings of the Third International Conference on Measuring Technology and Mechatronics Automation*.
[39] *Guidelines for Design of Wind Turbines*, 2002, Second Edition, Printed by Jydsk Centraltrykkeri, Denmark.
[40] Andersen L.V., Vahdatirad M.J., Sichani M.T., Sorensen J.D.,2012, Natural frequencies of wind turbines on mono pile foundations in clayey soils-A probabilistic approach, *Computers and Geotechnics* **43**: 1-11.
[41] Petersen B., Pollack M., Connell B., Greeley D., Daivis D., Slavik C., 2010, Evaluate the effect of turbine period of vibration requirements on structural design parameters, *Applied Physical Sciences Corp* 10-12.
[42] Schaumann P., Boker C., 2011, *Support Structures of Wind Energy Converters*, Springer, Wien New York.
[43] Sadeghi K., 2002, *Coasts, Ports and Offshore Structures Engineering*, Press of Water and Power University, First Edition.
[44] Taghipoor M., Qureshi Tayebi A., Lotfollahi yaghin A., 2005, Investigation of hydrodynamic forces on the roughness of the pile and compare it with candles, smooth and rough, *Proceedings of the First Congress on Civil Engineering*.
[45] Feyzollahzadeh M., Vibration analysis of offshore wind turbine on a monopile support structure, *Msc Thesis, Shahid Beheshti University*,Tehran.
[46] Bir G., Jonkman J., 2008, Modal dynamics of large wind turbines with different support structures, *Proceedings of the International Conference on Offshore Mechanics and Arctic Engineering*.
[47] *Recommended Practice for Planning, Designing and Constructing Fixed Offshore Platforms Working Stress Design*, 2000, API Recommended Practice, 2A-WSD.
[48] Jonkman J., Butterfield S., Passon P., Larsen T., Camp T., Nichols J., Azcona J., Martinez A., 2008, Offshore code comparison collaboration within IEA wind annex XXIII: phase II results regarding monopile foundation modeling, *NREL/CP-500-42471, National Renewable Energy Laboratory*.
[49] Han M., Benaroya H., Wei T., 1999, Dynamics of transversely vibrating beams using four engineering theories, *Journal of Sound and vibration* **5**: 935-988.
[50] Wu J., Chen C., 2007, Forced vibration analysis of an offshore tower carrying an eccentric tip mass with rotary Inertia due to support excitation, *Ocean Engineering* **34**: 1235-1244.
[51] Zhang Y., , Liu Y., , Chen P., Murphy K.D., 2011, Buckling loads and eigen frequencies of a branced beam resting on elastic foundation, *Acta Mechanica Solida Sinica* **24**: 510-518.
[52] Parvanova S., 2011, *Beams on Elastic Foundation*, University of Architecture, Civil Engineering and Geodesy Sofia, 111-125.
[53] Feyzollahzadeh M., Yadavar Nikravesh M., Rahi A., 2013, Dynamic analysis of offshore wind turbine tower using the transfer matrix method, *Proceedings of the 9th International Energy Conference*.
[54] Jonkman J., Musial W., 2010, Offshore code comparison collaboration (OC3), Final Technical Report, *NREL/TP-5000-48191, National Renewable Energy Laboratory*.
[55] Passon P., 2006, *Memorandum: Derivation and Description of the Soil-Pile-Interaction Models*, IOP Publishing Physics, IEA-Annex XXIIII Subtask 2, Stuttgart, Germany.
[56] Devriendt C., Jordaens P., Ingelgem Y. V., Sitter G. D., Guillaume P., 2012, *Monitoring of Resonant Frequencies and Damping Values of an Offshore Wind Turbine on a Monopile Foundation*, Offshore Wind Infrastructure, IOP Publishing Physics.
[57] *General Specification V90 – 3.0 MW Variable Speed Turbine*, 2004, Item no. 950010.R1, IOP Publishing Physics.